ISSN 1392 - 1207. MECHANIKA. 2013 Volume 19(1): 40-45

Human body rheology impact on measurements in accelerometer applications

V. Benevičius*, V. Ostaševičius, R. Gaidys*****

**Kaunas University of Technology, Studentų 65, 51369 Kaunas, Lithuania, E-mail: vincas.benevicius@gmail.com*
***Kaunas University of Technology, Studentų 65, 51369 Kaunas, Lithuania, E-mail: vytautas.ostasevicius@ktu.lt*
****Kaunas University of Technology, Studentų 65, 51369 Kaunas, Lithuania, E-mail: rimvydas.gaidys@ktu.lt*

crossref http://dx.doi.org/10.5755/j01.mech.19.1.3626

1. Introduction

Micro-electro-mechanical systems (MEMS) technology is at the center of enormous industry combining many different engineering disciplines & physics. One of MEMS technology outcome is accelerometer which has high potential for use in 3D movement analysis systems of any moving body: they are small, light, very easy to use and do not need to be attached to a reference and provide a signal which incorporates acceleration and inclination information. However, the analysis of 3D movements from accelerometer data is generally not straightforward.

One of the accelerometer applications is energy expenditure calculation during various physical activities. Although the idea of energy expenditure calculation using acceleration data is not new [1-3], studies still show relatively large errors. As accelerometers are mounted on the skin surface, they share a common problem – movement of the soft tissues covering the bones which is the source of errors [4-6]. We believe that these artifacts are the source of significant errors that can be avoided by incorporating human body rheological model into the equation of energy expenditure estimation. Such hypothesis can be supported by number of works where it is known that the skin mounted accelerometer is to be firmly attached to the skin with a preload compressing the soft tissue and increasing the stiffness of the sensor attachment in order to obtain accurate measurements and minimizing sensor mass. Although this is applicable in controlled environments, it is highly avoidable from the mass consumer point of view.

In order to prove given hypothesis several experiments were conducted. First, running – walking analysis was performed to obtain acceleration ranges and acceleration signal frequencies in a number of body points. Obtained values then were examined in order to make sure selected sensor's usage is valid. Later on, accelerometer's measurement quality in the obtained frequency range was analyzed. After that another experiment was conducted in order to identify movement differences between bone-fixed point and skin-mounted point in order to support our hypothesis. These differences then were inserted into walking speed, running speed and energy expenditure calculation to show how much of the impact human body rheology can have in such application.

2. Experimental setup

Complete research was performed through three experiments:

- walking-running analysis to obtain acceleration ranges and acceleration signal frequencies in different body places;
- chosen accelerometer's measurement analysis to obtain measurement characteristics;
- human body rheology experiment to identify movement differences between bone-fixed and skin-mounted points.

Fig. 1 ProReflex MCU 500 Type 170 214 camera

First experiment was conducted using 6 ProReflex motion capture unit (MCU) 500 Type 170 241 cameras (Fig. 1) with Qualisys Track Manager Software from Qualisys and Treadmill Vision Fitness Premier model T9450 HRT. The ProReflex MCU uses a 680×500 pixel charge-coupled device (CCD) image sensor. The use of CCD technology results in very low-noise data compared to a higher resolution complementary metal-oxide-semiconductor (CMOS) sensor which has a considerably higher pixel noise level. By using a patented sub-pixel interpolation algorithm, the effective resolution of the ProReflex MCU is 20000×15000 subpixels in a normal setup, enabling the ProReflex MCU to discern motions as small as 50 μm.

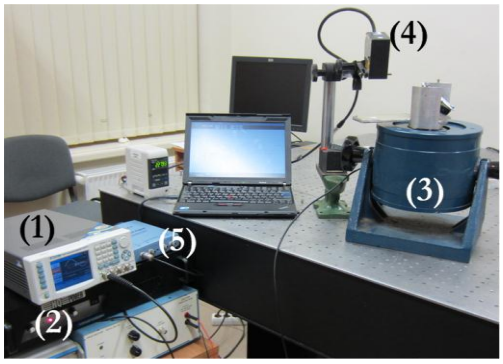

Fig. 2 Second phase experimental setup

Second experiment was conducted using following equipment (Fig. 2):

1 - frequencies generator Tabor Electronics WW5064 50Ms/s;
2 - power amplifier VPA2100MN;
3 - vibration stand Veb Robotron Type 11077;
4 - displacement measurement unit laser Keyence LK-G82 with controller Keyence LK-GD500;
5 - ADC Picoscope 3424.

Third experiment was conducted using 6 ProReflex MCU 500 Type 170 241 cameras (Fig. 1) with Qualisys Track Manager Software from Qualisys.

3. Experimental procedures

There are number of methods and places where small devices with the accelerometer inside can be attached on the human body in physical activity monitoring applications. Depending on actual application such devices can be worn:

- in a waist area using belt clip or they can simply lay on the bottom of the side or back pocket (like most pedometers and activity counters are worn);
- on chest using special belts (common for heart rate monitors) or as an integrated part in the clothes (emerged with growing applications of smart textiles);
- on biceps using special Velcro strap pouches (quite common for some types of activity monitors or Global Positioning System (GPS) based tracking devices);
- on wrist using clock-like attachments (common for heart rate monitors and locomotion counters);
- on thigh or tarsus using special straps or pouches (common for running, walking monitoring or gait analysis devices).

Such wide variety of attachment options has evolved from different application requirements as well as end user comfort and usability requirements. Waist, chest and tarsus are attractive places for the device to be attached in physical activity monitoring applications as dynamics of these areas strongly correlate with everyday activities and ordinary motion as walking and running. Mentioned places are also highly appealing for the end-users as the devices there usually do not pose any movement restrictions and are comfortable to wear. Combined with emerging smart textile technologies these devices can compose small wearable systems that can be worn unnoticed by the external viewer and provide comfort level of casual underwear people wear every day. Such level of comfort expands physical activity monitoring to the new horizons allowing physical activities to be tracked 24/7 for long periods of time.

Walking-running analysis was performed to obtain acceleration ranges and acceleration signal frequencies in all mentioned places – chest, back, biceps, hips, wrists, thighs and tarsi – and makes a set of 7 attachment points. Two males participated in the experiment. Although such small test subject set might raise doubts about experiment results, it is not the case as two test subjects are enough to evaluate acceleration characteristics. We do not make any conclusions on specific values rather than trend.

Experiments started with slow 0.8 km/h walking, was gradually increased to 13 km/h intensive running and decreased back to 0.8 km/h (Fig. 3). Speed was changed in increments/decrements of 0.1 km/h width delay of 5 seconds. Three cycles were performed for each test subject.

Fig. 3 Test subject with tracking markers walking on the treadmill

All motion data (position x, y and z) was captured with data sampling rate of 500 Hz to keep raw data at maximum resolution that was allowed by the hardware. All captured data was filtered using 20 Hz low pass filter with 80dB attenuation at 25 Hz as bandwidth of 20 Hz is where natural human movements occur (10-16 Hz values can be seen in literature).

Filtered data was down sampled to 50 Hz yet keeping the band of interest undistorted (Nyquist theorem allows that as our bandwidth is 20 Hz while sampling frequency is left 50 Hz which is two times more than the bandwidth). Residual analysis was performed with filtered data to define differentiator filter pass band frequency and resulted in 16 Hz pass band frequency. Differentiator filter was applied twice on each data set to acquire accelerations.

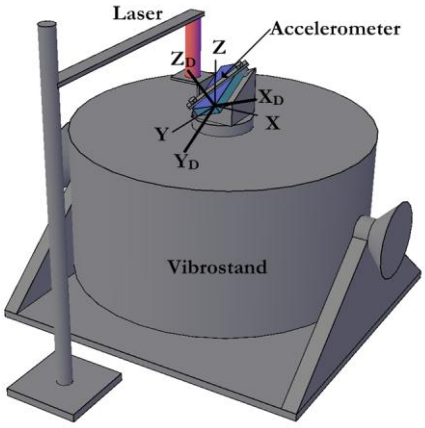

Fig. 4 Accelerometer mounting on the vibrostand; (x, y, z) – global coordinate system; (X_D, Y_D, Z_D) – accelerometer's coordinate system

During second experiment device with accelerometer was mounted the way that all accelerometer's angles would be around 45° with GPS (Fig. 4). This was done in order to excite all three accelerometer axes at once. Frequencies fed to vibrostand were 1, 4 , 7 , 10 , 14 , 17 and 20 Hz to cover whole band of interest (20 Hz). Two runs were done with every frequency. Vibrostand displacement data was recorded using ADC Picoscope 3424 with 10 kHz data sampling rate ant accelerometer's signal was sampled at 400 Hz sampling rate.

Collected vibrostand displacement data was filtered with 50 Hz low pass filter with full stop frequency at

250 Hz, then down sampled 20 times to sampling frequency of 500 Hz. Then 30 Hz (full stop at 50 Hz) differentiator was used to calculate accelerations. On the other hand acceleration data was filtered with 30 Hz low pass filter with full stop set to 50 Hz. Vibration axis data was obtained by averaging axes data from 10 , 14, 17 and 20 Hz experiments where measured acceleration signals showed high linearity in 3D space (Fig. 5).

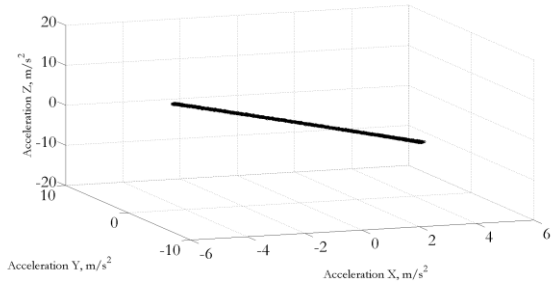

Fig. 5 Measured acceleration 3D plot that clearly shows vibration axis

Then all data was rotated using 3D rotation matrix so the vibration axis would match accelerometer's z axis. Finally input signal was compared to measured values.

During third experiment four points were tracked (Fig. 6). One was rigidly mounted to the forehead to display skeleton movement (fixed point); other three were mounted on the device (loose points, Fig. 7) with accelerometer inside to track device movement.

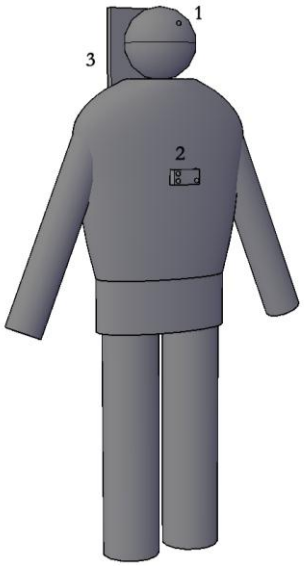

Fig. 6 Experiment setup on the body: *1* – forehead tracking point, *2* – device with *3* tracking points (anticlockwise) *3* – woodchip board to rigidly fix head to the body in order to remove neck movement

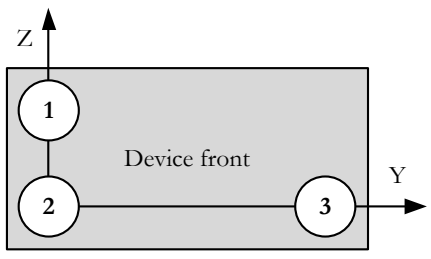

Fig. 7 Markers' configuration on the device

The device itself was attached to the belt which was placed around the chest (Fig. 6). During experiment test subject was vertically jumping with different intensities. Data was collected, fixed and loose points' movement were compared. Trajectory sampling rate was 100 Hz.

Residual analysis was performed with measured data sets to identify low pass filter pass band frequency. The filter then was used to filter measured movement trajectories of all 4 points (Fig. 6). In order to match jumping axis with measurement space Z axis, measurement data was rotated in space so two vertically positioned points on the device (Fig. 7) and z axis would match as close as possible.

4. Experiment related models

Two mathematical models were designed and modeling results were compared to experimental data. First model was dedicated to accelerometer. Its validity was showed in previous article of the authors [7]. Another model was dedicated to human body rheology (Fig. 6).

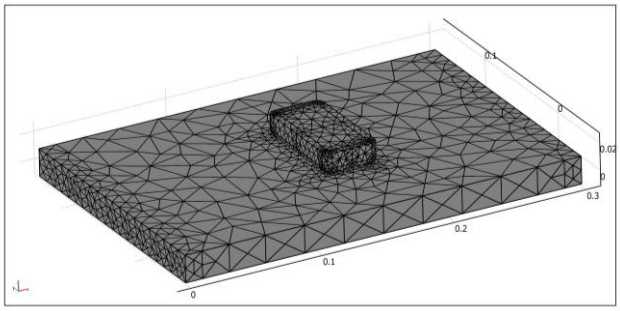

Fig. 6 Reduced human body model (chest area)

Model consists of two parts – device with initial prestress described as:

$$[K]\{u\} = \{F\} \tag{1}$$

and base's transient analysis with kinematic excitation. Material model of the device is isotropic elastic material having density of 806 kg/m^3. The size of the device is 80×40×16 mm.

The base is reduced human body model having properties of the actual human body. Material model is hyper elastic Neo-Hookean with initial shear modulus of 100 Pa, initial bulk modulus of 1000 Pa and density of 1000 kg/m^3.

All modeling was conducted with Comsol Multiphysics.

In the considered finite element (FE) formulation the dynamics of the reduced human body model is described by the following equation of motion in a block form by taking into account that base motion law is known and is defined by the nodal displacement vector $\{U_K(t)\}$

$$\begin{bmatrix}[M_{NN}] & [M_{NK}]\\ [M_{KN}] & [M_{KK}]\end{bmatrix}\begin{Bmatrix}\{\ddot{U}_N\}\\ \{\ddot{U}_K\}\end{Bmatrix}+\begin{bmatrix}[C_{NN}] & [C_{NK}]\\ [C_{KN}] & [C_{KK}]\end{bmatrix}\begin{Bmatrix}\{\dot{U}_N\}\\ \{\dot{U}_K\}\end{Bmatrix}+$$
$$+\begin{bmatrix}[K_{NN}] & [K_{NK}]\\ [K_{KN}] & [K_{KK}]\end{bmatrix}\begin{Bmatrix}\{U_N\}\\ \{U_K\}\end{Bmatrix}=\begin{Bmatrix}\{0\}\\ \{R\}\end{Bmatrix}, \tag{2}$$

where nodal displacement vectors $\{U_N(t)\},\{U_K(t)\}$ correspond to displacements of free nodes and kinematically excited nodes respectively; $[M]$, $[C]$, $[K]$ are mass, damping and stiffness matrices respectively; $\{R\}$ is a vector representing reaction forces of the kinematically excited nodes.

Displacement vector of unconstrained nodes is expressed as $\{U_N\} = \{U_{Nrel}\} + \{U_{Nk}\}$, where $\{U_{Nrel}\}$ denotes a component of relative displacement with respect to moving base displacement $\{U_{Nk}\}$. Vectors $\{U_K\}$ and $\{U_{Nk}\}$ correspond to rigid-body displacements which do not induce internal elastic forces in the structure. Proportional damping approach is adopted in the form $[C] = \alpha[M] + \beta[K]$ with α and β as Rayleigh damping constants. Hence, the following matrix equation is obtained after the algebraic rearrangements of previous equations:

$$\left[M_{NN}\right]\left\{\ddot{U}_{Nrel}\right\}+\left[C_{NN}\right]\left\{\dot{U}_{Nrel}\right\}+\left[K_{NN}\right]\left\{U_{Nrel}\right\}=\left[\hat{M}\right], \quad (3)$$

where the equation contains matrices of the structure constrained in the nodes of imposed kinematic excitation, and:

$$\left[\hat{M}\right]=\left[M_{NN}\right]\left[K_{NN}\right]\left[K_{NK}\right]-\left[M_{NK}\right], \quad (4)$$

represents a vector of inertial forces that act on each node of the structure as a result of applied kinematic excitation.

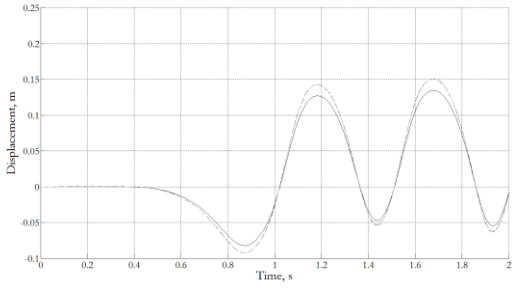

Fig. 7 Modeling results – dashed line – is well aligned with modeling results – dotted line: curves match

The kinematic excitation was imposed on the boundary in terms of displacement vector $\{U_K(t)\}$.

As can be seen in the Fig 9, designed model fits experimental data. Observed error was less than 5%. These two mathematical models can be combined together to get acceleration measurements in virtual environment taking into consideration human body rheological properties. This way reversed problem can be successfully solved: what bone movement would be if accelerometer measurements are known.

5. Results and discussion

All displacement experimental data clearly shows that body movements for walking/running and similar activities fall into bandwidth of 20 Hz. This way most part of high frequency non-movement related noise can be removed with low pass filters.

Experimental data also suggest safe acceleration limits for the hardware that is used to capture acceleration data during walking/running and similar type of activities. As industrial accelerometers have ranges $\pm 2g$, $\pm 4g$, $\pm 6g$, $\pm 8g$, $\pm 16g$, it is suggested to use $\pm 8g$ for torso where measured accelerations reached up to 50 m/s^2 and $\pm 16g$ for limbs where measured accelerations reached up to 96 m/s^2.

A Table 1 below shows that measurement error for frequencies over 7 Hz gives error up to 11%. Lower frequencies tend to give bigger errors because of the low acceleration values thus the device operates near its SNR limit.

It‘s must be said that actual body movement is of much greater amplitudes. It means that low frequency movement still results in higher acceleration levels and the device can operate further from its signal-to-noise ratio (SNR). This way error levels decrease to acceptable limits even with frequencies up to 7 Hz in real life measurements. Taking this into consideration we concluded that given accelerometer LIS3LV02DLH is sufficient for body movement measurements.

Table 1

Accelerometer measurements compared to excitation data

Vibrostand frequency, Hz	Vibrostand displacement amplitude, mm	Vibrostand acceleration amplitude, m/s^2	Accelerometer measured amplitude, m/s^2	Error
1	0.8813	0.0348	0.0452	30%
4	0.9517	0.6012	0.6914	15%
7	0.9510	1.8397	2.0435	11%
10	1.0822	4.2725	4.5236	6%
14	1.0335	7.9967	8.1595	2%
17	0.9891	11.2849	11.0833	2%
20	0.9241	14.5920	13.8016	5%

Filtered and rotated 3D displacement data of 4 tracked points were compared in between (Fig. 8). As expected, distances between all three points that were mounted on the device were constant during all experiment. However, distances between forehead point and device points varied with time (Fig. 8 and Fig. 9).

These figures give the base for a very important conclusion: because of human body rheological properties device movement on the chest compared to the movement on the forehead (as a solid attachment to the spine) can differ as high as 3 cm while making simple non intensive vertical jumping (Fig. 9). This means human body rheological properties plays important role and strongly impacts measurements.

Walking speed, running speed and energy expenditure formulas were developed and published in Journal of Vibroengineering [8].

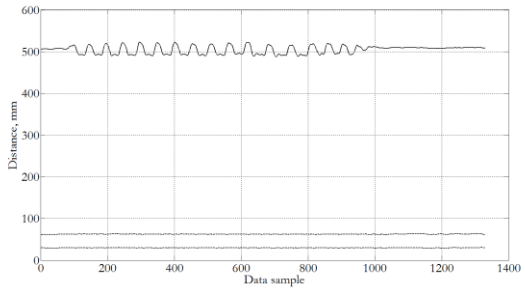

Fig. 8 Distances between pairs of points (from top to bottom): forehead marker – device marker 2, device marker 1 – device marker 2, device marker 3 – device marker 2 (for markers' positions refer to Fig. 6 and Fig. 7)

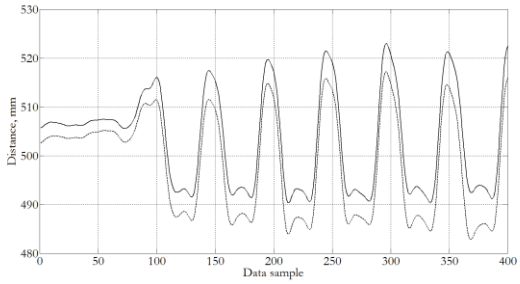

Fig. 9 Distance and z coordinate (vertical) differences between forehead marker and device marker 2 (Fig. 7)

Table 2

A comparison of results received with and without human body rheological properties impact

Activity	a_z	v_w	v_r	MET_w	MET_r
Walking (1)	0.22	4.93	–	5.73	–
Walking (2)	0.27	6.13	–	6.91	–
Difference (3)	–	+24.3%	–	+20.6%	–
Running (1)	0.91	–	11.13	–	10.44
Running (2)	0.99	–	14.30	–	11.27
Difference (3)	–	–	+28.5%	–	+8.0%

(1) – no human body rheology impact;
(2) – human body rheology impact is present;
(3) – difference was calculated as ((2) – (1) / (1)) × 100 %

Walking speed:

$$v_w = -18.736a_z^2 + 24.754a_z + 0.3898. \quad (5)$$

Running speed:

$$v_r = 51.535a_z^2 - 58.322a_z + 21.527. \quad (6)$$

Energy expenditure (*EE*):

$$EE = MET \times weight(kg) \times duration(h), \quad (7)$$

where MET (Metabolic Equivalent of Task) while walking:

$$MET_w = 14.662a_z + 2.5083 \quad (8)$$

and MET while running:

$$MET_r = 10.318a_z + 1.053. \quad (9)$$

Following given equations a table of calculated speeds and energy expenditure values were set up in order to compare results when accelerations are measured without and with human body rheological properties impact (Table 2).

Results clearly indicate strong human body rheology impact into acceleration based application (in this case walking and running speed and energy expenditure) outcome. Given numbers shows that in running application predicted walking speed increased from 4.93 km/h when no human body rheology impact was present to 6.13 km/h when human body rheology was present giving total increase of 24.3%. The increase of 28.5%was even greater in running application but this is expected as the movement is more intense while running thus gives bigger skin surface movements.

6. Conclusions

1. It is suggested that for the hardware that is used to capture acceleration data during walking/running and similar type of activities ±8*g* measurement range should be used for torso and ±16*g* for limbs.

2. Chosen hardware LIS3LV02DLH is sufficient for walking, running and similar types of activities acceleration measurement (up to 11% error is expected).

3. For walking and running application human body rheology can be the source of 24.3% increase in predicted walking speed and the source of 28.5% increase in predicted running speed.

Acknowledgements

This research was funded by a grant (No. 31V-16) from the Lithuanian Agency of Science, Innovation and Technology.

References

1. **Garcia, A.W.; Langenthal, C.R.; Angulo-Barroso, R.M.; Gross, M.M.** 2004. A comparison of accelerometers for predicting energy expenditure and vertical groud reaction force in school-age children, Measurement in Physical Education and Exercise Science 8(3): 119-144. http://dx.doi.org/10.1207/s15327841mpee0803_1.
2. **King, G.A.; Torres, N.; Potter, C.; Brooks T.J.;**

Coleman, K.J. 2004. Comparison of activity monitors to estimate energy cost of treadmill exercise. Medicine & Science in Sports & Exercise 37(7): 1244-1251. http://dx.doi.org/10.1249/01.MSS.0000132379.09364.F8.

3. **Crouter, S.E.; Clowers, K.G.; Bassett, Jr.D.R.** 2006. A novel method for using accelerometer data to predict energy expenditure, Journal of Applied Physiology 100: 1324-1331. http://dx.doi.org/10.1152/japplphysiol.00818.2005.
4. **Chiari, L.; Della Croce, U.; Leardini, A.; Cappozzo, A.** 2005. Human movement analysis using stereophotogrammetry, Part 2: Instrumental Errors. Gait and Posture 21: 197-211. http://dx.doi.org/ 10.1016/j.gaitpost.2004.04.004.
5. **Cappozzo, A.; Della Croce, U.; Leardini, A.; Chiari, L.** 1996. Position and orientation in space of bones during movement: experimental artefacts, Clinical Biomechanics 11: 90-100. http://dx.doi.org/10.1016/0268-0033(95)00046-1.
6. **Lucchetti, L.; Cappozzo, A.; Cappello, A.; Della Croce, U.** 1998. Skin movement artifact assessment and compensation in the estimation of knee-joint kinematics, Journal of Biomechanics 31: 977-984. http://dx.doi.org/10.1016/S0021-9290(98)00083-9.
7. **Benevicius, V.; Ostasevicius, V.; Venslauskas, M.; Dauksevicius, R.; Gaidys, R.** 2011. Finite element model of MEMS accelerometer for accurate prediction of dynamic characteristics in biomechanical applications, Journal of Vibroengineering 13(4): 803-809.
8. **Satkunskienė, D.; Grigas, V.; Eidukynas, V.; Domeika, A.** 2009. Acceleration based evaluation of human walking and running parameters, Journal of Vibroengineering 11(3): 506-510.

V. Benevičius, V. Ostaševičius, R. Gaidys

ŽMOGAUS KŪNO REOLOGIJOS ĮTAKA AKCELEROMETRIJA PAREMTIEMS TAIKYMAMS

R e z i u m ė

Straipsnyje pateikiama hipotezė apie žmogaus kūno reologinių savybių įtaką pagreičio matavimo rezultatams ir galimus iškraipymus galutiniuose taikymo rezultatuose, kurią bandoma pagrįsti atliekant tris eksperimentus, sudarant matematinį modelį bei parodant taikymo rezultatų iškraipymą. Pirmo eksperimento pagalba tiriamos 7-ių kūno taškų pagreičių charakteristikos, antrojo pagalba įrodoma, jog pasirinkta įranga yra tinkama tokio uždavinio taikyme, trečiojo pagalba parodoma žmogaus kūno reologinių savybių įtaka galimiems matavimams. Straipsnyje taip pat pateikiamas sudarytas redukuotas žmogaus kūno dalies (krūtinės zonos) reologinis modelis, parodomas jo adekvatumas eksperimento duomenims. Galiausiai parodoma, jog žmogaus kūno reologinių savybių įtaka yra ženkli rezultatams, kurie gaunami naudojant pagreičio matavimo duomenis.

V. Benevičius, V. Ostaševičius, R. Gaidys

HUMAN BODY RHEOLOGY IMPACT ON MEASUREMENTS IN ACCELEROMETER APPLICATIONS

S u m m a r y

Article present and tries to prove hypothesis that human body rheological properties can have significant impact on results that are based on accelerometry in biomechanical applications. Three experiments are conducted, mathematical model is developed and real world application is shown to support given hypothesis. During first experiment analysis of 7 body points' acceleration characteristics is conducted. During the second experiment it is show that selected hardware (accelerometer LIS3LV02DLH) is sufficient in such applications. During third experiment it is show that human body rheology has impact on acceleration measurements in real world application. Article also presents simplified human body model (chest area) and shows its adequacy to experiment data. Finally, it is shown how much human body rheology impact real world accelerometry based calculations.

Keywords: human body rheological properties, accelerometer, body FEM, biomechanics.

Received March 02, 2012
Accepted February 11, 2013